a special exception to the general rule that target selection by developing axons is independent of neural activity.

References and Notes

1. C. S. Goodman and C. J. Shatz, *Neuron* **10**, 77 (1993); C. J. Shatz and D. D. M. O'Leary, *Arch. Ophthalmol.* **111**, 472 (1993); L. C. Katz and C. J. Shatz, *Science* **274**, 1133 (1996).
2. K. L. Allendoerfer and C. J. Shatz, *Annu. Rev. Neurosci.* **17**, 185 (1994); N. Konig, G. Roch, R. Marty, *Anat. Embryol.* **148**, 73 (1975); D. Kristt, *ibid.* **157**, 217 (1979); I. Kostovic and P. Rakic, *J. Neurocytol.* **9**, 219 (1980); F. Valverde, M. Facal-Valverde, M. Santacana, M. Heredia, *J. Comp. Neurol.* **290**, 118 (1989).
3. A. Ghosh and C. J. Shatz, *J. Neurosci.* **12**, 39 (1992).
4. E. Friauf, S. K. McConnell, C. J. Shatz, *ibid.* **10**, 2601 (1990); K. Herrmann, A. Antonini, C. J. Shatz, *Eur. J. Neurosci.* **6**, 1729 (1994).
5. E. Friauf and C. J. Shatz, *J. Neurophysiol.* **66**, 2059 (1991); R. Wong, M. Meister, C. J. Shatz, *Neuron* **11**, 923 (1993); R. Mooney, A. Penn, R. Gallego, C. J. Shatz, *ibid.* **17**, 863 (1996).
6. All animal care was in accordance with institutional guidelines. A total of 25 fetuses (E56, $n = 22$; E42, $n = 3$) were studied from pregnant cats in our breeding colony of known gestational age. Anesthesia, sterile surgical techniques, and minipump implantations were according to (*22*). After infusion of either 300 μM TTX or vehicle (300 μM sodium citrate buffer) between E42 and E56, the fetuses were delivered by cesarean section and were transcardially perfused (*3*). Fetuses are always studied as littermate pairs (TTX-treated compared with vehicle-treated) because TTX diffuses throughout the entire forebrain and midbrain bilaterally (*9*), and therefore it is not possible to compare hemispheres in the same animal.
7. Crystals of DiI (D-282, Molecular Probes, Eugene, OR) were placed into either the subplate or cortical plate of visual cortex to label LGN neurons that project there or into the LGN itself to visualize the axonal projection from LGN to cortex. In the same animals, crystals of DiD (D-7757, Molecular Probes) were also placed into the region of auditory cortex to label LGN axons that might extend collaterals into this region on their way back to visual cortex. After 3 months for dye diffusion, brains were sectioned horizontally on a vibratome at 100 μm, and retrogradely labeled LGN neurons were counted. Because the number of retrogradely labeled neurons is directly proportional to the size of the dye injection site, great care was taken to make similar dye injection sizes for each TTX- and vehicle-treated littermate pair ($n = 11$ matched littermate pairs studied). The variations in total neuron number seen in Fig. 1, C and D, reflect differing size injections, and therefore comparisons can only made between matched littermate pairs.
8. Infusion of vehicle did not have an apparent effect on the magnitude of the LGN projection to visual cortex; the number of retrogradely labeled LGN neurons was within 10% (± 2% SEM, $n = 3$ unmanipulated and 3 vehicle-treated; $P < 0.005$) of untreated littermate controls matched for similar injection sizes.
9. Previous studies have demonstrated that intracranial minipump infusions of TTX produce concentrations that are sufficient to block sodium-dependent action potentials bilaterally throughout the entire forebrain and midbrain at E42 to E56 (*22*) and result in the failure of retinal ganglion axons to segregate into eye-specific layers in the LGN (*17, 23*). However, many other aspects of development proceed normally: Cell migration and cell division within the cortex are unimpaired, the brain grows to normal size during the treatment period and its gross histological organization is indistinguishable from normal (*23*), and the somatic and dendritic development of retinal ganglion cells and LGN neurons is normal [(*22*); M. Dalva, A. Ghosh, C. J. Shatz, *J. Neurosci.* **14**, 3588 (1994)]. Moreover, the development of cortical pyramidal cell dendrites, radial glial cells, and the overall appearance and thickness of the cortical plate is indistinguishable from normal (*12*).
10. TTX infusions were begun at E42, after large numbers of MGN axons had already invaded the auditory cortical plate [A. Ghosh and C. J. Shatz, *Development* **117**, 1031 (1993)].
11. S. M. Catalano and C. J. Shatz, data not shown.
12. K. Herrmann and C. J. Shatz, *Proc. Natl. Acad. Sci. U.S.A.* **92**, 11244 (1995).
13. TTX- or vehicle-treated littermate pairs with small dye placements (2 to 3 mm^3) in identical cortical locations were analyzed for topographic precision ($n = 4$ pairs) (Fig. 3). The location of individual labeled LGN neurons with respect to the borders of the LGN was marked on digitized images of sections. The mediolateral distribution of marked neurons within a single section was plotted in 100-μm bin widths (NIH Image version 1.61). This procedure was repeated for every LGN section. The distributions for all sections were added together, and the peak number of retrogradely labeled neurons was determined. Finally, the percentage of total mediolateral width of LGN covered by labeled neurons at half-peak was derived and plotted in Fig. 3B.
14. The peak in the number of retrogradely labeled neurons was located near the center of LGN in vehicle-treated animals (within 250 to 300 μm of the center of LGN), consistent with dye placements within the corresponding locations in visual cortex. However, in TTX-treated animals, the peak was located further medially in two cases and further laterally in one case (550 to 350 μm away from the center) than in vehicle-treated control littermates, even though the DiI injections were similarly placed in cortex, suggesting that there is more variability in the overall topography of the geniculocortical projection after TTX treatment.
15. J. T. Schmidt and M. Buzzard, *J. Neurobiol.* **21**, 900 (1990); U. Drescher *et al.*, *Cell* **82**, 359 (1995); M. Nakamoto *et al.*, *ibid.* **86**, 755 (1996).
16. The normal increase between E42 and E56 in the number of LGN neurons projecting to visual cortex, as determined by retrograde labeling with DiI injections, is about 30-fold ($n = 3$ untreated animals at E42 and 3 vehicle-treated animals at E56).
17. D. W. Sretavan, C. J. Shatz, M. P. Stryker, *Nature* **336**, 468 (1988).
18. D. K. Simon, G. T. Prusky, D. D. M. O'Leary, M. Constantine-Paton, *Proc. Natl. Acad. Sci. U.S.A.* **89**, 10593 (1992); H. Cline, *Trends Neurosci.* **14**, 104 (1991); M. D. Olson and R. L. Meyer, *J. Neurosci.* **14**, 208 (1994).
19. It is conceivable that TTX somehow disrupts cortical differentiation, which in turn affects LGN axon targeting and ingrowth. Although this disruption is possible, we note that many aspects of cortical development can proceed normally after similar TTX treatments; see (*9*).
20. M. Tessier-Lavigne, *Cell* **82**, 345 (1995).
21. A. Ghosh, A. Antonini, S. K. McConnell, C. J. Shatz, *Nature* **347**, 179 (1990); Z. Molnar and C. Blakemore, *ibid.* **351**, 475 (1991); J. A. De Carlos and D. D. M. O'Leary, *J. Neurosci.* **12**, 1194 (1992); J. Bolz, N. Novak, V. Staiger, *ibid.*, p. 3054.
22. G. Campbell, A. S. Ramoa, M. P. Stryker, C. J. Shatz, *Visual Neurosci.* **14**, 779 (1997).
23. C. J. Shatz and M. P. Stryker, *Science* **242**, 87 (1988).

24. We thank A. Raymond and D. Escontrias for help with the fetal surgeries. Supported by NIH grant EY02838 (C.J.S.) and National Research Service Award EY06491 (S.M.C.). S.M.C. is an Associate and C.J.S. is an Investigator of the Howard Hughes Medical Institute.

12 March 1998; accepted 10 June 1998

A Viral Mechanism for Inhibition of the Cellular Phosphatase Calcineurin

James E. Miskin, Charles C. Abrams, Lynnette C. Goatley, Linda K. Dixon*

The transcription factor NFAT (nuclear factor of activated T cells) controls the expression of many immunomodulatory proteins. African swine fever virus inhibits proinflammatory cytokine expression in infected macrophages, and a viral protein A238L was found to display the activity of the immunosuppressive drug cyclosporin A by inhibiting NFAT-regulated gene transcription in vivo. This it does by binding the catalytic subunit of calcineurin and inhibiting calcineurin phosphatase activity.

Viruses encode many proteins that interfere with host defense systems (*1*). Nucleotide sequence analysis of the African swine fever virus (ASFV) genome (*2*) identified genes encoding proteins that are potentially able to interfere with the host response to viral infection. These include A238L, which has sequence similarity with IκB, and prevents activation of nuclear factor kappa B (NF-κB)–dependent gene transcription (*3*). The similarity between A238L and IκB is limited to the central region of the protein, which contains three ankyrin-like repeats. The NH_2- and COOH-terminal regions of A238L are unlike those of the cellular IκB proteins (*4*), indicating that A238L may function by means of a mechanism different from that of IκB.

To identify host proteins with which A238L interacts, we used the yeast two-hybrid system (*5, 6*) to screen a cDNA library from pig alveolar macrophages. Nine clones specifically interacted with A238L, including four containing cDNA encoding the entire porcine cyclophilin A (*CypA*) gene. Another four clones contained cDNAs encoding all but the first 30 to 40 NH_2-terminal amino acid residues of the catalytic (A) subunit of the Ca^{2+}-calmodulin–regulated cellular phospha-

Institute for Animal Health, Pirbright Laboratory, Pirbright, Surrey, GU24 0NF, UK. E-mail: linda.dixon@bbsrc.ac.uk

*To whom correspondence should be addressed.

tase calcineurin (CaN). The A238L homolog from the virulent Malawi (LIL20/1) ASFV isolate also interacted with CaN and CypA. CaN and CypA interacted with A238L specifically, with no binding to the unrelated Gal4 DNA binding domain fusions SNF1 (*5*) and CDK2 (*7*). The CaN-A238L interaction was also detected when the genes were fused to the alternative domains of Gal4. The immunosuppressive drug cyclosporin A (CsA) binds to CypA, and this complex binds to and inhibits the activity of CaN (*8*). We postulate that A238L might function as a protein analog of CsA and inhibit the activity of CaN, either alone or as an A238L-CypA complex.

To confirm the interaction between A238L and CaN, we tested for in vitro binding of these proteins (*9*) (Fig. 1). In vitro–translated A238L, IκB, or an irrelevant ASFV protein (I14L) was immunoprecipitated with antibodies to epitope tags [SV5 or hemagglutinin (HA)] fused to these genes. Purified CaN added before immunoprecipitation was coprecipitated with A238L but not with the other proteins; it was detected by an antiserum that recognizes both the CaN A and B subunits (Fig. 1B) or by antiserum to the B subunit [anti-CaN(B)] (Fig. 1D). With the anti-CaN(B) we detected binding of endogenous CaN to SV5-A238L (Fig. 1D). CaN coprecipitated with A238L in the absence of added CypA, but we cannot exclude a requirement for CypA in the reaction, given that small amounts of CypA are present in the in vitro translation mixes (*10*). The A238L-CaN interaction was unaffected by a high concentration of CsA (10 μM) (Fig. 1B), implying that A238L either interacts with CaN at a different site from the CsA-CypA complex or can displace CsA–CypA complexes.

We tested for the interaction between A238L and CaN under physiological conditions by analyzing proteins from extracts of ASFV-infected cells that coimmunoprecipitated with A238L (*11*). A recombinant ASFV was constructed (SV5-A238L) in which the

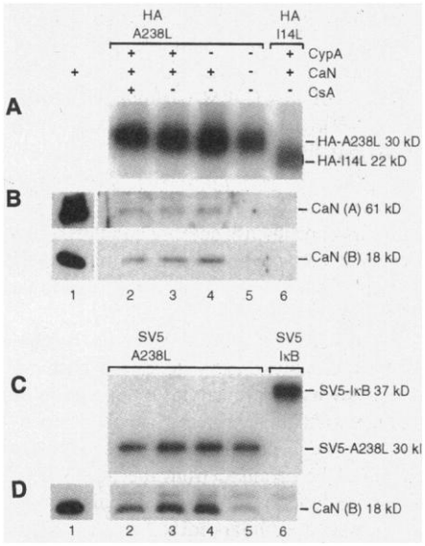

Fig. 1. Direct binding of A238L to CaN in vitro (*9*). In vitro–translated HA-A238L (lanes 2 through 5) or HA-I14L (lane 6) was mixed with CaN (2 μg; lanes 2, 3, 4, 6), CypA (2 μg; lanes 2, 3, 6), and CsA (10 μM; lane 2). Mixtures were incubated with 2 μg of HA-specific monoclonal antibody, and the immune complexes were collected on protein A–Sepharose beads before separation by SDS–polyacrylamide gel electrophoresis (PAGE). Purified CaN (100 ng, lane 1) was run in parallel. Immunoprecipitated proteins were detected by autoradiography (**A**) or by protein immunoblot analysis with polyclonal anti-CaN (**B**). In vitro–translated SV5-A238L (lanes 2 through 5) and SV5-IκB (lane 6) were mixed with CaN (2 μg; lanes 2, 3, 4, 6), CypA (2 μg; lanes 2, 3, 6), and CsA (10 μM; lane 2). Purified CaN (50 ng, lane 1) was run in parallel. Mixtures were incubated with 5 μg of SV5-specific antibody, and the immune complexes were collected and analyzed by autoradiography (**C**) or by protein immunoblot analysis with monoclonal antibody to CaN(B) (**D**).

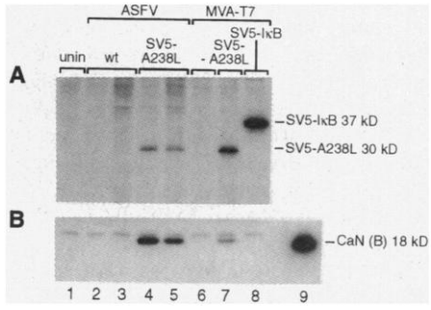

Fig. 2. Coprecipitation of CaN and A238L from cells (*11*). Vero cells were uninfected (lane 1), infected with wild-type BA71V ASFV for 4 (lane 2) or 10 hours (lane 3), or infected with SV5-A238L ASFV for 4 (lane 4) or 10 hours (lane 5). BSC1 cells were infected with MVA-T7 and transfected with vector alone (lane 6), pT7–SV5–A238L (lane 7), or pT7–SV5-IκB (lane 8). Purified CaN (50 ng) was run in parallel (lane 9). Radiolabeled cell extracts were immunoprecipitated with monoclonal anti-SV5, immune complexes were separated by SDS-PAGE, and immunoprecipitated proteins were detected by autoradiography (**A**) or by protein immunoblot analysis with monoclonal antibody to CaN(B) (**B**).

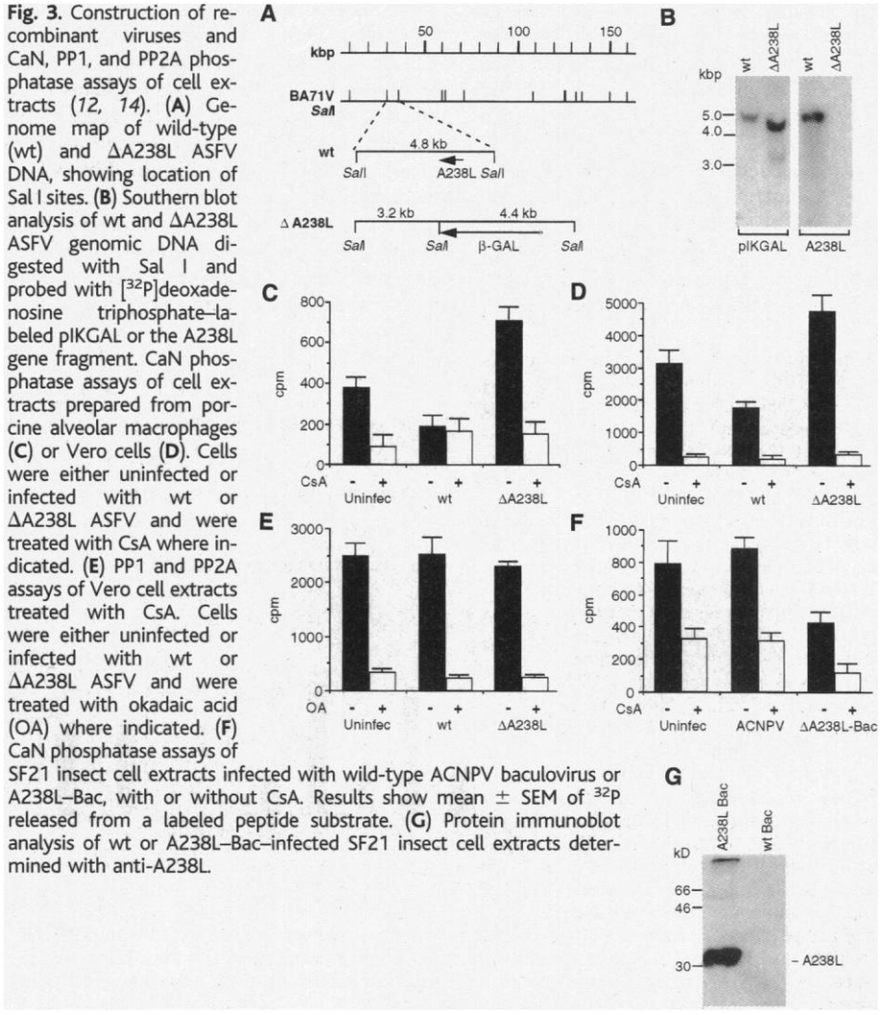

Fig. 3. Construction of recombinant viruses and CaN, PP1, and PP2A phosphatase assays of cell extracts (*12, 14*). (**A**) Genome map of wild-type (wt) and ΔA238L ASFV DNA, showing location of Sal I sites. (**B**) Southern blot analysis of wt and ΔA238L ASFV genomic DNA digested with Sal I and probed with [^{32}P]deoxadenosine triphosphate–labeled pIKGAL or the A238L gene fragment. CaN phosphatase assays of cell extracts prepared from porcine alveolar macrophages (**C**) or Vero cells (**D**). Cells were either uninfected or infected with wt or ΔA238L ASFV and were treated with CsA where indicated. (**E**) PP1 and PP2A assays of Vero cell extracts treated with CsA. Cells were either uninfected or infected with wt or ΔA238L ASFV and were treated with okadaic acid (OA) where indicated. (**F**) CaN phosphatase assays of SF21 insect cell extracts infected with wild-type ACNPV baculovirus or A238L–Bac, with or without CsA. Results show mean ± SEM of ^{32}P released from a labeled peptide substrate. (**G**) Protein immunoblot analysis of wt or A238L–Bac–infected SF21 insect cell extracts determined with anti-A238L.

A238L open reading frame (ORF) was tagged at the NH_2-terminus with the SV5 epitope (*12*). Synthesis of the SV5-A238L protein was detected 4 hours after infection (Fig. 2A), as previously reported (*13*). CaN was coprecipitated with SV5-tagged A238L in SV5-A238L ASFV–infected cell extracts but not in the controls (Fig. 2B). Radiolabeled, SV5-tagged A238L or IκB was transiently expressed in BSC1 cells (Fig. 2A); CaN coprecipitated with SV5-A238L but not with SV5-IκB (Fig. 2B), showing that the A238L-CaN interaction is specific.

To study the effect of A238L on CaN phosphatase activity, we constructed a recombinant ASFV (ΔA238L) in which the A238L-coding region was deleted (Fig. 3A) (*12*). Removal of the A238L gene was confirmed by Southern (DNA) blot analysis (Fig. 3B) (*12*). The growth characteristics of ΔA238L and wild-type ASFV BA71V in Vero cells were the same (*10*).

CaN phosphatase activity was assayed in extracts from primary porcine alveolar macrophages (Fig. 3C) and Vero cells (Fig. 3D) that were either uninfected or infected with wild-type or ΔA238L ASFV (*14*). The assays were specific for CaN; CsA reduced the phosphatase activity (Fig. 3, C and D). Macrophages and Vero cells infected with wild-type ASFV contained about half as much CaN activity as the uninfected cells. In macrophages, ASFV infection reduced CaN activity to the background level observed in the presence of CsA (Fig. 3C). In ΔA238L-infected cells, CaN activity was two to three times that of wild-type–infected cells, demonstrating that expression of A238L inhibits CaN activity. CaN activity was higher in ΔA238L-infected cells than in uninfected cells, which suggests that, although ASFV infection may increase CaN activity, A238L counteracts this effect. The amount of CaN in both cell extracts was the same (*10*). The activity of the other major Ser-Thr protein phosphatases (PP1 and PP2A) was similar in uninfected cells and in cells infected with wild-type ASFV or ΔA238L, indicating that A238L inhibits CaN specifically (Fig. 3E). CaN activity was also reduced about one-half (Fig. 3F) by A238L in insect cells that had been infected with a recombinant baculovirus expressing A238L (A238L-Bac) (*12, 14*) (Fig. 3G).

CaN is a ubiquitously expressed phosphatase with diverse functions. One substrate is the NFAT (nuclear factor of activated T cells) family of transcription factors, to which CaN directly binds (*15*). Inhibition of CaN activity by the CsA–CypA complex (or by the FK506–FKBP12 complex) prevents NFAT activation by inhibiting CaN-dependent dephosphorylation of the cytoplasmically located subunit of NFAT (*16*). This prevents its nuclear translocation as well as the transcription of NFAT-dependent genes, which include immunomodulatory cytokines.

CaN inhibition by A238L in ASFV-infected macrophages might prevent activation of an NFAT factor, thus preventing transcription of the immunomodulatory genes that depend on NFAT. Using a porcine macrophage cDNA library, we identified by polymerase chain reaction (PCR) and nucleotide sequence analysis an amplified fragment similar to NFATc (GenBank U08015), which displayed 86.1% nucleotide identity and 94.2% amino acid identity (Fig. 4A) (*17*). We also identified (by reverse transcriptase-PCR and nucleotide sequence analysis) an amplified fragment from porcine RS-2 cells similar to NFAT1 (Genbank U43341), displaying 91.1% nucleotide identity and 100% amino acid identity (Fig. 4A) (*17*).

Cotransfection of a vector expressing A238L with an NFAT-dependent reporter gene cassette in RS-2 cells consistently (n = 5) reduced reporter gene expression to 50 to 60% of that of the vector only (pCDNA3) controls (Fig. 4B) (*18*). The A238L homolog from the LIL20/1 ASFV isolate also reduced NFAT-dependent reporter gene expression, whereas the vector expressing an irrelevant ASFV gene (l14L) had no effect (*10*). Reporter gene expression was undetected using a construct in which the NFAT-binding sites had been mutated (*10, 18*). Reduction of NFAT-driven gene transcription by A238L was specific; reporter gene expression from a construct containing AP-1–binding sites was unaffected by either expression of A238L or treatment with CsA (Fig. 4C) (*18*).

A238L also inhibits NF-κB–dependent gene transcription (*3*). However, inhibition of CaN activity cannot explain the reduction of NF-κB activation by A238L in cells treated with PMA alone (*3*). PMA-stimulated activation of NF-κB is not inhibited by CsA, which shows that this pathway is not CaN-dependent (*10, 19*). Therefore, A238L seems to have two functions: first, to bind to CaN and inhibit its phosphatase activity and thus CaN-dependent pathways; second, to inhibit NF-κB–dependent transcription by an unknown mechanism.

A238L may provide a versatile mechanism that enables ASFV to evade host defense systems by preventing transcription of immunomodulatory proteins, which is dependent on NFAT or NF-κB. Virus genes are thought to be captured from the host and to mimic the function of host genes; the implication is that cellular homologs of A238L exist.

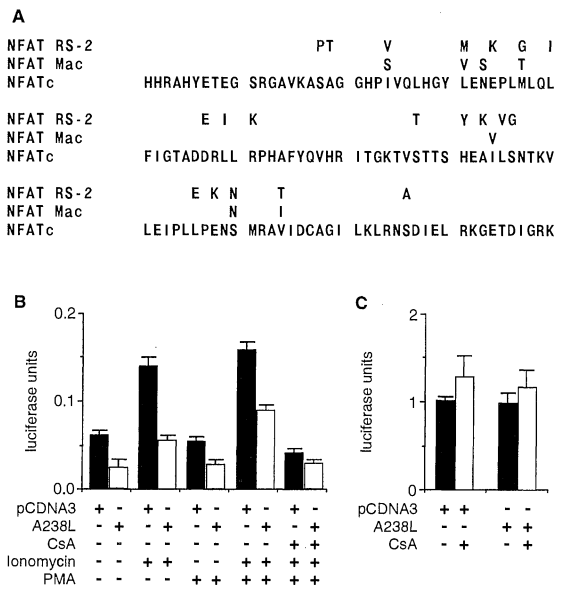

Fig. 4. Sequence comparison of porcine NFAT-like sequences and the effect of A238L on the expression of an NFAT-dependent luciferase reporter gene (*17, 18*). (**A**) Amino acid sequence comparison between human NFATc (amino acids 437 to 556; U08015), a porcine macrophage NFAT gene fragment (NFAT Mac; AF069996), and a porcine RS-2 cell NFAT gene fragment (NFAT RS-2; AF069995); only residues that differ from the NFATc sequence are shown. Abbreviations for the amino acid residues are as follows: A, Ala; C, Cys; D, Asp; E, Glu; F, Phe; G, Gly; H, His; I, Ile; K, Lys; L, Leu; M, Met; N, Asn; P, Pro; Q, Gln; R, Arg; S, Ser; T, Thr; V, Val; W, Trp; and Y, Tyr. (**B**) An NFAT-luc reporter plasmid was cotransfected with pCDNA3 or pCDNA3–A238L into RS-2 cells treated with the indicated compounds. By 24 hours after transfection, the cells were harvested and luciferase activity was assayed. (**C**) An AP-1 luc reporter plasmid was cotransfected with pCDNA3 or pCDNA3–A238L into RS-2 cells. All cells were treated with ionomycin and phorbol 12-myristate 13-acetate (PMA), and some were treated with CsA (as indicated). Cells were harvested and assayed for luciferase activity. Data represent mean ± SEM.

References and Notes

1. N. J. Davispoynter and H. E. Farrell, *Immunol. Cell. Biol.* **74**, 513 (1996); A. Alcami and G. L. Smith, *Immunol. Today* **16**, 474 (1995).
2. R. J. Yanez *et al.*, *Virology* **208**, 249 (1995); L. K. Dixon *et al.*, *J. Gen. Virol.* **75**, 1655 (1994).
3. P. P. Powell, L. K. Dixon, R. M. E. Parkhouse, *J. Virol.* **70**, 8527 (1996).
4. P. A. Baeuerle and D. Baltimore, *Cell* **87**, 13 (1996); A. S. Baldwin Jr., *Ann. Rev. Immunol.* **14**, 649 (1996).
5. S. Fields and O.-K. Song, *Nature* **340**, 245 (1989); T. Durfee *et al.*, *Genes Dev.* **7**, 555 (1993).
6. A porcine alveolar macrophage cDNA library in λACT2 (*5*) was cotransformed with A238L cloned in pGBT9 (Clontech) in yeast strain Y190. Clones encoding interacting proteins were selected on medium lacking histidine and by expression of β-galactosidase (β-Gal). The sequence of inserts was determined.
7. J. W. Harper, G. R. Adami, N. Wei, K. Keyomarsi, S. J. Elledge, *Cell* **75**, 805 (1993).
8. S. L. Schreiber and G. R. Crabtree, *Immunol. Today* **13**, 136 (1992).
9. A238L and I14L were tagged with the influenza virus HA epitope; A238L and IκB with the simian virus 5

(SV5) epitope [T. Hanke, P. Szawlowski, R. E. Randall, *J. Gen. Virol.* **73**, 653 (1992)] in pCDNA3 (Invitrogen). In vitro–translated, radiolabeled proteins were mixed with 2 μg of CaN (Sigma), 2 μg of CypA (Sigma) and 10 μM CsA (Sandoz) where appropriate, absorbed with protein A–Sepharose (Sigma), and immunoprecipitated with 2 μg of anti-HA (Boehringer) or 5 μg of anti-SV5 (Serotec). Complexes were analyzed by autoradiography or protein immunoblot analysis with polyclonal anti-CaN (Chemicon) or monoclonal anti-CaN(B) (Sigma).

10. J. E. Miskin, C. C. Abrams, L. K. Dixon, unpublished observations.
11. Vero cells were infected with wild-type BA71V ASFV or SV5-A238L recombinant ASFV (*12*) for 4 to 10 hours. BSC1 cells were infected with modified vaccinia ankara (MVA) expressing T7 RNA polymerase [G. Sutter, M. Ohlmann, V. Erfle, *FEBS Lett.* **371**, 9 (1995)] and transfected with pT7–SV5-A238L or pT7–SV5-IκB. Proteins were radiolabeled, and the lysed cell extracts were immunoprecipitated and analyzed as before (*9*).
12. Regions flanking the A238L ORF were cloned into KS vector (Stratagene), and the β-Gal gene downstream from the ASFV vp72 promoter [J. M. Rodriguez, F. Almazan, E. Vinuela, J. F. Rodriguez, *Virology* **188**, 67 (1992)] was cloned between them. In addition, SV5-tagged A238L was cloned downstream from the A238L promoter. Recombinant ASF viruses ΔA238L and SV5-A238L were isolated by using X-Gal (5-bromo-4-chloro-3-indoxyl-β-D-galactopyranoside). Recombinant baculovirus expressing A238L (A238L–Bac) was constructed with use of the BAC TO BAC baculovirus expression system (Life Technologies). Anti-A238L was raised in rabbits by using bacterially expressed A238L purified by SDS-polyacrylamide gel–electrophoresis.
13. J. G. Neilan *et al.*, *Virology* **235**, 377 (1997).
14. D. A. Fruman, S.-Y. Pai, C. B. Klee, S. J. Burakoff, B. E. Bierer, in *Methods: Companion Methods Enzymol.* **9**, 146 (1996).
15. C. Loh *et al.*, *J. Biol. Chem.* **271**, 10884 (1996).
16. K. T.-Y. Shaw *et al.*, *Proc. Natl. Acad. Sci. U.S.A.* **92**, 11205 (1995); A. Rao, C. Luo, P. G. Hogan, *Annu. Rev. Immunol.* **15**, 707 (1997).
17. Messenger RNA from RS-2 cells was converted to cDNA by using anchored oligo dT_{25}. PCR-amplified fragments corresponding to nucleotides 1309 to 1669 of the NFATc ORF (GenBank U08015) were cloned into pT7-Blue2 (Novagen), and the nucleotide sequence was determined.
18. The A238L ORF was cloned in pCDNA3. The reporter plasmids used were NFAT-luc, mutant NFAT-luc (mNFAT-luc), and AP-1-luc. Transfected RS-2 cells were treated after 16 hours with (where appropriate) 40 nM PMA (Sigma), 4 μM ionomycin (Sigma), and 1 μM CsA (Sandoz), and luciferase activity was assayed 24 hours later.
19. B. Franz *et al.*, *EMBO J.* **13**, 861 (1994); T. Kanno and U. Siebenlist, *J. Immunol.* **157**, 5277 (1996).
20. We thank S. J. Elledge for two-hybrid reagents; R. Hay for pT7-SV5-IκB; G. R. Crabtree for the NFAT-luc reporter plasmid; E. McKenzie, I. O'Beirne, and A. Lennard for mNFAT-luc and AP-1-luc; and Sandoz Pharmaceuticals for CsA. Supported by the Biotechnology and Biological Sciences Research Council and Ministry of Agriculture Fisheries and Food.

10 April 1998; accepted 8 June 1998

Delivery of Epitopes by the *Salmonella* Type III Secretion System for Vaccine Development

Holger Rüssmann,* Homayoun Shams, Fernando Poblete, Yixin Fu, Jorge E. Galán,† Ruben O. Donis

Avirulent strains of *Salmonella typhimurium* are being considered as antigen delivery vectors. During its intracellular stage in the host, *S. typhimurium* resides within a membrane-bound compartment and is not an efficient inducer of class I–restricted immune responses. Viral epitopes were successfully delivered to the host-cell cytosol by using the type III protein secretion system of *S. typhimurium*. This resulted in class I–restricted immune responses that protected vaccinated animals against lethal infection. This approach may allow the efficient use of *S. typhimurium* as an antigen delivery system to control infections by pathogens that require this type of immune response for protection.

The success of global vaccination programs requires efficacious vaccines that are stable and easy to administer (*1*). Viable carrier systems offer the greatest potential for innovative approaches to develop polyvalent vaccines. Efficient protection against infectious agents often requires the action of both humoral and cellular immune mechanisms. Therefore, an ideal polyvalent antigen delivery system should be capable of stimulating all desired effector cell populations of the immune system. Live replicating bacteria and viruses that stimulate complex immune responses have been rendered avirulent and endowed with the ability to express foreign proteins derived from pathogenic microorganisms (*2*). Avirulent strains of *Salmonella typhimurium* are being widely considered as delivery systems for heterologous antigens because of their ability to induce complex mucosal and systemic immune responses after oral administration (*3*). A characteristic feature of these bacteria is their ability to invade nonphagocytic cells such as those of the intestinal epithelium (*4*). After internalization, *S. typhimurium* remains confined to a membrane-bound compartment insulated from the cytosolic environment of the host cell (*5*). Localization within the "internalization" vacuole prevents delivery of expressed foreign antigens to the major class I antigen presentation pathway, thereby hampering the use of *Salmonella* vaccine carriers when this type of response is crucial for protection (for example, viral infections) (*6*). An attempt to circumvent this problem has been the use of *Salmonella* to deliver plasmid DNA to express antigens within the host-cell cytosol (*7*).

Contact of *S. typhimurium* with host cells results in activation of a specialized protein secretion system (type III) that is encoded in a pathogenicity island at centisome 63 of its chromosome (*4*). This protein secretion system delivers a set of bacterial effector proteins into the host-cell cytosol, which leads to stimulation of signal transduction pathways that result in a variety of responses such as actin cytoskeleton reorganization and activation of transcription factors (*4*). In an effort to improve the ability of *Salmonella* to elicit class I–restricted immune responses to those epitopes, we investigated the potential of this system to deliver heterologous epitopes into the host-cell cytosol. To this end, we chose SptP, a *S. typhimurium* effector protein that is delivered into the host cell through the centisome 63 type III secretion system but is not required for efficient bacterial entry into nonphagocytic cells (*8*). We constructed a chimeric form of SptP that carries a class–I restricted epitope consisting of residues 366 to 374 from the influenza virus nucleoprotein ($IVNP_{366–374}$) found to be immunodominant in mice of the *H-2*^{b} haplotype (*9*). The epitope was introduced at a permissive site of SptP (*10*) located between the two predicted independent domains of this protein (Fig. 1) (*8*). The chimeric SptP-$IVNP_{366–374}$ protein was secreted into the culture supernatant of both wild-type *S. typhimurium* and the isogenic avirulent *aroA sptP* mutant strain SB824 at concentrations indistinguishable from those of wild-type SptP (Fig. 1). Both strains efficiently delivered SptP-$IVNP_{366–374}$ into the cytosol of infected cultured epithelial cells (Fig. 1). In contrast, and as expected, the isogenic *S. typhimurium sipD* mutant strain SB221 did

H. Rüssmann, Y. Fu, J. E. Galán, Department of Molecular Genetics and Microbiology, School of Medicine, State University of New York at Stony Brook, Stony Brook, NY 11794–5222, USA. H. Shams, F. Poblete, R. O. Donis, Department of Veterinary and Biomedical Sciences, University of Nebraska-Lincoln, Lincoln, NE 68583–0905, USA.

*Present address: Max von Pettenkofer-Institut, Pettenkofer Strasse 9a, 80336 Munich, Germany.
†To whom correspondence should be addressed. E-mail: galan@asterix.bio.sunysb.edu